Plant Biotechnology Journal
Open Access

Plant Biotechnology Journal (2022) **20**, pp. 564–576 doi: 10.1111/pbi.13738

Mutant combinations of *lycopene ε-cyclase* and *β-carotene hydroxylase 2* homoeologs increased β-carotene accumulation in endosperm of tetraploid wheat (*Triticum turgidum* L.) grains

Shu Yu, Michelle Li[a], Jorge Dubcovsky and Li Tian*

Department of Plant Sciences, University of California, Davis, CA, USA

Received 14 May 2021;
revised 21 October 2021;
accepted 22 October 2021.
**Correspondence* (Tel +1 530 7520940;
Fax: +1 530 7529659;
email ltian@ucdavis.edu)

[a]Codexis Inc., Redwood City, CA, USA

Keywords: Wheat, carotenoid, lutein, lycopene ε-cyclase, β-carotene, β-carotene hydroxylase, provitamin A biofortification, grain, endosperm.

Summary

Grains of tetraploid wheat (*Triticum turgidum* L.) mainly accumulate the non-provitamin A carotenoid lutein—with low natural variation in provitamin A β-carotene in wheat accessions necessitating alternative strategies for provitamin A biofortification. Lycopene ε-cyclase (LCYe) and β-carotene hydroxylase (HYD) function in diverting carbons from β-carotene to lutein biosynthesis and catalyzing the turnover of β-carotene to xanthophylls, respectively. However, the contribution of *LCYe* and *HYD* gene homoeologs to carotenoid metabolism and how they can be manipulated to increase β-carotene in tetraploid wheat endosperm (flour) is currently unclear. We isolated loss-of-function Targeting Induced Local Lesions in Genomes (TILLING) mutants of *LCYe* and *HYD2* homoeologs and generated higher order mutant combinations of *lcye-A*, *lcye-B*, *hyd-A2*, and *hyd-B2*. *Hyd-A2 hyd-B2*, *lcye-A hyd-A2 hyd-B2*, *lcye-B hyd-A2 hyd-B2*, and *lcye-A lcye-B hyd-A2 hyd-B2* achieved significantly increased β-carotene in endosperm, with *lcye-A hyd-A2 hyd-B2* exhibiting comparable photosynthetic performance and light response to control plants. Comparative analysis of carotenoid profiles suggests that eliminating *HYD2* homoeologs is sufficient to prevent β-carotene conversion to xanthophylls in the endosperm without compromising xanthophyll production in leaves, and that β-carotene and its derived xanthophylls are likely subject to differential catalysis mechanisms in vegetative tissues and grains. Carotenoid and gene expression analyses also suggest that the very low *LCYe-B* expression in endosperm is adequate for lutein production in the absence of *LCYe-A*. These results demonstrate the success of provitamin A biofortification using TILLING mutants while also providing a roadmap for guiding a gene editing-based approach in hexaploid wheat.

Introduction

Carotenes and their oxygenated derivatives, xanthophylls, are carotenoid molecules recognized for their critical roles in photosynthesis and photoprotection (Shumskaya and Wurtzel, 2013). Carotenoids with at least one unmodified β-ionone ring (aka. provitamin A carotenoids), such as β-vcarotene, can also be used to form vitamin A that is essential for vision and immune functions but cannot be synthesized *de novo* in humans (Britton, 2009; Mora *et al*., 2008). There is great interest in improving the provitamin A content of food crops to alleviate the health burden of vitamin A deficiency caused by a lack of dietary intake (Yu and Tian, 2018). Some notable efforts include the genetic engineering of β-carotene production in rice endosperm in first and second generations of Golden Rice, and the breeding of high β-carotene maize varieties (Harjes *et al*., 2008; Paine *et al*., 2005; Yan *et al*., 2010; Ye *et al*., 2000).

As one of the most widely cultivated staple crop in the world, grains of tetraploid durum and hexaploid common wheat serve as an important source of proteins and calories for humans despite their low accumulation of provitamin A carotenoids (Yu and Tian, 2018). In contrast to hexaploid wheat that generally lacks carotenoids in their grain endosperm, tetraploid wheat grains accumulate lutein in the endosperm, where it is a main contributor to grain yellow pigment content (GYPC)—a quality trait preferred by consumers. Lycopene ε-cyclase (LCYe) constitutes a key control point for the continuation of lycopene to lutein or β-carotene biosynthesis and is tightly associated with a major effect quantitative trait loci (QTL) for GYPC in wheat (Howitt *et al*., 2009) (Figure 1a). Violaxanthin, a xanthophyll derived from β-carotene, accumulates in developing tetraploid wheat endosperms, suggesting that β-carotene produced in the endosperm is further modified by β-carotene hydroxylase (HYD) and then epoxidase activities (Qin *et al*., 2016) (Figure 1a). Homoeologs of two *HYDs*, *HYD1,* and *HYD2*, were isolated from tetraploid and hexaploid wheat and all functioned towards β-carotene in an *E. coli* system (Qin *et al*., 2012).

In diploid and autopolyploid plant species, increased accumulation of β-carotene in storage tissues was achieved by suppressing the activities of LCYe to reallocate carbon flux from lutein to β-carotene, and/or HYD(s) to decrease the conversion of β-carotene to xanthophylls, such as those reported in potato tubers (Diretto *et al*., 2006, 2007), maize kernels (Harjes *et al*., 2008; Yan *et al*., 2010), and *Brassica*

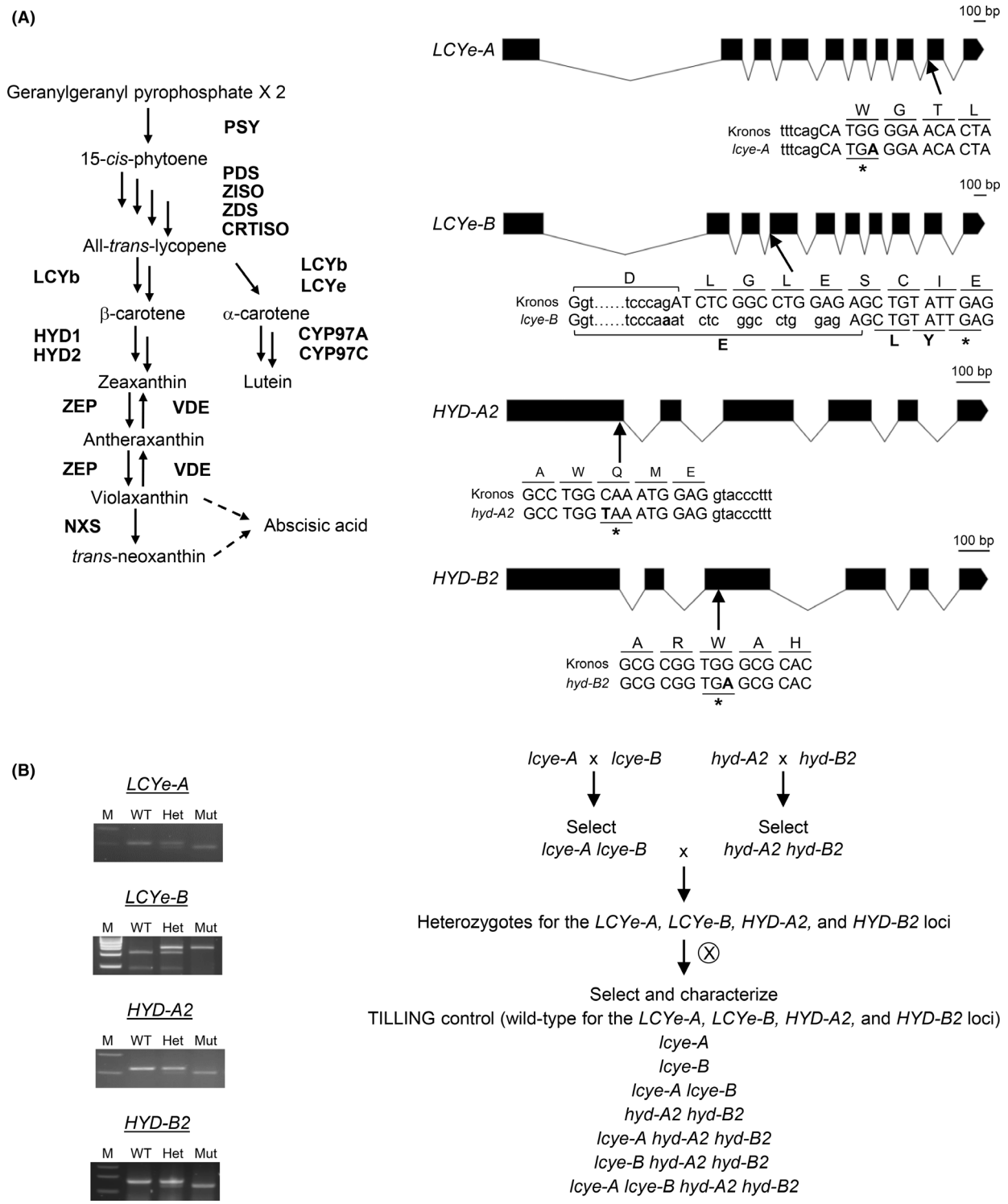

Figure 1 Isolation of *lcye-A*, *lcye-B*, *hyd-A2*, and *hyd-B2* TILLING mutants in tetraploid wheat and generation of higher order mutant combinations. (a) A simplified scheme of carotenoid biosynthetic pathway in higher plants. Dashed arrows denote multiple reaction steps. PSY, phytoene synthase; PDS, phytoene desaturase; ZISO, 15-*cis*-ζ-carotene isomerase; ZDS, ζ-carotene desaturase; CRTISO, carotenoid isomerase; LCYb, lycopene β-cyclase; LCYe, lycopene ε-cyclase; HYD, β-carotene hydroxylase; ZEP, zeaxanthin epoxidase; VDE, violaxanthin de-epoxidase; NXS, neoxanthin synthase. (b) Intron-exon organization of *LCYe-A*, *LCYe-B*, *HYD-A2*, and *HYD-B2*. Exons are shown in boxes and introns are indicated with lines. Mutated nucleotides and amino acids/premature stop codons in the *lcye-A*, *lcye-B*, *hyd-A2*, and *hyd-B2* mutants used in this study are highlighted in bold. *: stop codon. (c) CAPS and dCAPS markers for *LCYe-A*, *LCYe-B*, *HYD-A2*, and *HYD-B2*. PCR amplification products of each gene homoeolog from wild-type and mutant plants were digested with the corresponding restriction enzymes shown in Table S6 and separated on a 2.5% agarose gel. M, DNA size marker; WT, wild-type plant; Het, heterozygous mutant plant; Mut, homozygous mutant plant. (d) A schematic diagram of generation and selection of mutant combinations used in this study. x, crossing; ⊗, self-pollination.

napus seeds (Yu *et al*., 2008). Although the general strategy of manipulating *LCYe* and *HYDs* can be applied to allopolyploid wheat for improving grain β-carotene content, the presence and (distinct) function of multiple homoeologs of these carotenoid metabolic genes necessitate careful dissection to ensure successful deployment of provitamin A biofortification strategies. To this end, the expression of *LCYe*, *HYD1*, and *HYD2* homoeologs were analyzed in pericarp, embryo, and endosperm sections of developing grains as well as leaf, root, and stem of tetraploid and hexaploid wheat (Qin *et al*., 2016). *LCYe-A*, *HYD-A2*, and *HYD-B2* were the only *LCYe, HYD1*, and *HYD2* homoeologs with detectable expression by real-time qPCR in developing endosperms of tetraploid wheat, suggesting they play a role in endosperm carotenoid metabolism. By contrast, the transcript levels of *LCYe*, *HYD1*, and *HYD2* homoeologs were comparable in the embryo, pericarp, and vegetative tissues (Qin *et al*., 2016).

To understand the *in planta* function of LCYe homoeologs, loss-of-function Targeting Induced Local Lesions in Genomes (TILLING) mutants of *LCYe-A* and *LCYe-B* homoeologs were isolated (Richaud *et al*., 2018; Sestili *et al*., 2019) and crossed to generate *lcye-A lcye-B* (Sestili *et al*., 2019). Whole grains of *lcye-A lcye-B* showed a dramatic reduction of lutein, but only led to a slight increase in β-carotene. Because whole grains, not grain endosperms (i.e. flour), were analyzed for *lcye-A*, *lcye-B*, and *lcye-A lcye-B*, it is unclear how *lcye-A* and *lcye-B* mutations could affect specifically endosperm carotenoids in tetraploid wheat (Richaud *et al*., 2018; Sestili *et al*., 2019). It also remains unknown how changes to HYD, specifically HYD2, activity will affect tetraploid wheat endosperm carotenoid profiles.

To determine the individual and combined effects of *LCYe* and *HYD2* mutations on β-carotene accumulation in tetraploid wheat grain endosperm, we isolated loss-of-function TILLING mutants of *LCYe* and *HYD2* homoeologs and generated double, triple, and quadruple mutant combinations of *lcye-A*, *lcye-B*, *hyd-A2*, and *hyd-B2* in this study. The *hyd-A2 hyd-B2*, *lcye-A hyd-A2 hyd-B2*, *lcye-B hyd-A2 hyd-B2*, and *lcye-A lcye-B hyd-A2 hyd-B2* mutants exhibited significantly increased β-carotene in grain endosperm. Molecular, biochemical, and physiological analyses of the mutant combinations also provided new insights into the complex control of carotenoid metabolism in tetraploid wheat grains.

Results

Tetraploid wheat TILLING mutants of LCYe and HYD2 homoeologs were identified and higher order mutant combinations generated

To assess the function of *LCYe* and *HYD2* homoeologs in carotenoid metabolism in wheat, mutants of *HYD-A2* (42), *HYD-B2* (54), *LCYe-A* (79), and *LCYe-B* (77) homoeologs were identified in a tetraploid wheat cv. Kronos TILLING mutant library that contains 1536 mutants (Krasileva *et al*., 2017) (number of mutant lines is indicated in parenthesis next to the gene homoeolog). Line T4-0870 (*hyd-A2*) contains a C to T mutation at position 337 of the open reading frame (ORF) (Q113*), leading to a premature stop codon and a truncated protein that is 182 amino acids shorter than the full length HYD-A2 (Figure 1b). Line T4-4420 (*hyd-B2*) contains a G to A mutation at position 447 of the ORF (W149*), resulting in a premature stop codon that shortens HYD-B2 by 151 amino acids (Figure 1b). These truncated HYD2 proteins lack the conserved histidine residues essential for HYD (non-heme di-iron protein) activities (Bouvier *et al*., 1998), thus leading to loss-of-function *hyd2* mutants.

Line T4-2426 (*lcye-A*) contains a G to A mutation at position 1311 of the ORF, introducing a premature stop codon (W437*) (Figure 1b). As a result, 98 amino acids are lacking from the C-terminus of the 534-amino acids LCYe-A, including a charged region and a complete transmembrane helix region demonstrated to be essential for the LCYe enzyme function (Cunningham *et al*., 1996; Richaud *et al*., 2018; Sestili *et al*., 2019). Unlike *hyd-A2*, *hyd-B2*, and *lcye-A*, mutants with premature stop codons resulting directly from point mutations were not identified for *LCYe-B* in the tetraploid wheat TILLING mutant library. However, line T4-2543 (*lcye-B*) contains a G to A mutation at the splice acceptor site in intron 2 of *LCYe-B*, resulting in an alternatively spliced transcript of *LCYe-B* with a frameshift in the ORF that leads to a premature stop codon (Figure 1b). As a result, 373 amino acids are missing and 3 amino acids are incorrectly translated towards the C-terminus of LCYe-B in *lcye-B* (Figure 1b).

As chemical mutagenesis typically induces multiple mutations in each TILLING mutant line, the *lcye-A*, *lcye-B*, *hyd-A2*, and *hyd-B2* mutants were backcrossed twice to the wild-type parental line Kronos to reduce about 75% of background mutations. Homozygous single, double, triple, and quadruple mutants of *LCYe* and *HYD2* homoeologs were identified with molecular markers designed to distinguish wild-type and mutant alleles of the individual homoeologs (Figure 1c) following the intercrossing and selection scheme outlined in Figure 1d. Plants that are homozygous wild type for the *LCYe-A*, *LCYe-B*, *HYD-A2*, and *HYD-B2* loci in the segregating population contain a similar percentage of background mutations as the mutant lines and were used as controls for the subsequent studies (designated TILLING control) (Figure 1d). The *lcye-A* and *lcye-B* mutants were analyzed together with the higher order mutant combinations for the analyses reported in this study. Unless specified, 'the mutants' collectively refers hereafter to the *lcye-A*, *lcye-B*, *lcye-A lcye-B*, *hyd-A2 hyd-B2*, *lcye-A hyd-A2 hyd-B2*, *lcye-B hyd-A2 hyd-B2*, and *lcye-A lcye-B hyd-A2 hyd-B2* mutants analyzed in this study. The mutants did not show differences in growth relative to TILLING control under the greenhouse growth condition (Figure 2a).

The lcye-A lcye-B and lcye-A lcye-B hyd-A2 hyd-B2 mutants displayed most drastic changes in carotenoid profiles in leaves and stems

To understand the function of *LCYe* and *HYD2* and their homoeologs in carotenoid biosynthesis in photosynthetic tissues, carotenoid content in leaves and stems of the mutants and

Figure 2 Plant growth and carotenoid profiles of TILLING control and mutants. (a) Two-month-old TILLING control and mutant plants. (b) Grains of TILLING control and mutant plants. Whole grains and polished whole grains (with embryos removed and pericarps polished) are shown. (c) Carotenoid extracts of polished grains harvested from TILLING control and mutant plants. (d) HPLC chromatograms of carotenoids extracted from leaves of 2-month-old plants. (e) HPLC chromatograms of carotenoids extracted from polished whole grains. 1. Neoxanthin; 2. Violaxanthin; 3. Unidentified peak; 4. Lutein; 5. Zeaxanthin; 6. Chlorophyll *b*; 7. Chlorophyll *a*; 8. β-carotene.

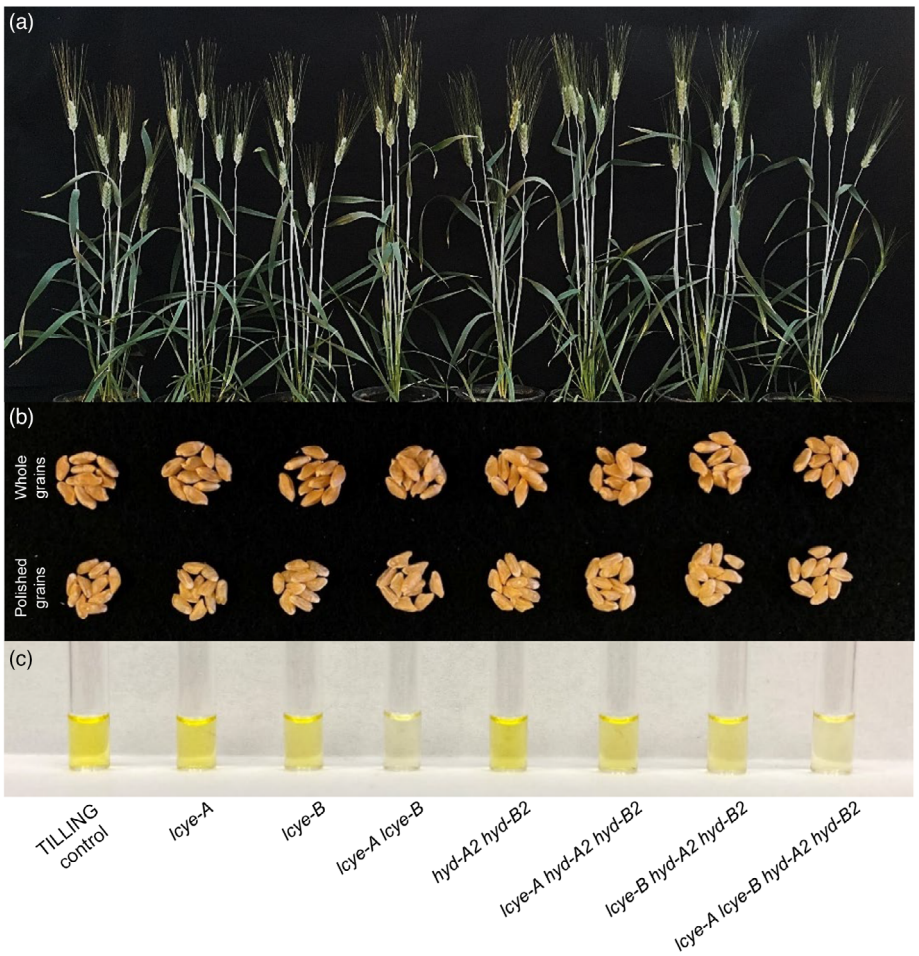

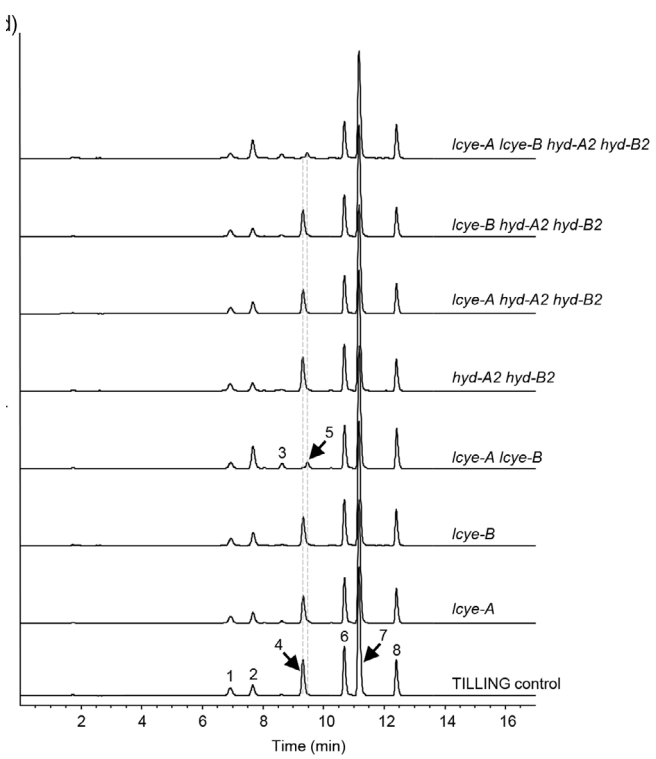

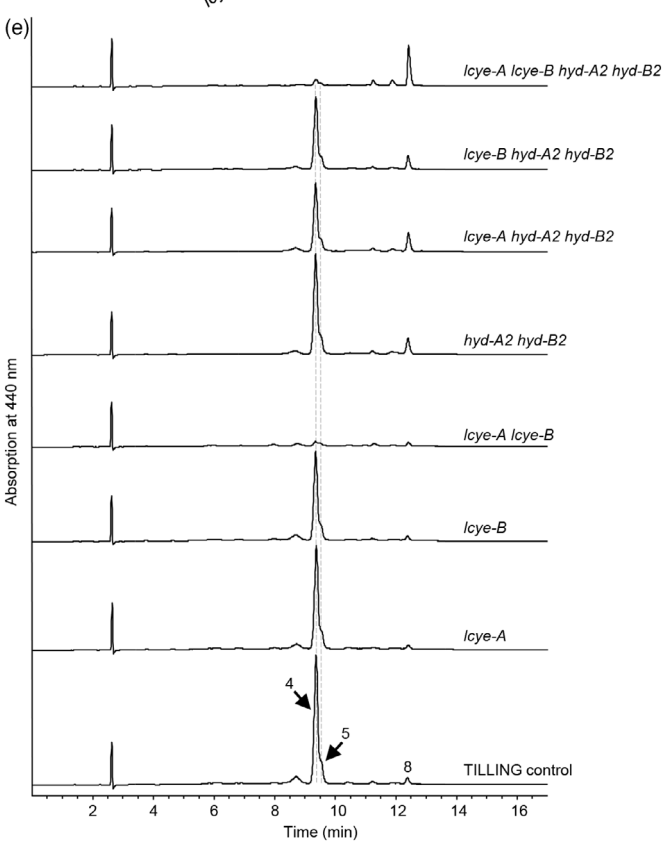

TILLING control were analyzed and compared (Figure 2d; Tables 1 and S1). Lutein (peak 4), β-carotene (peak 8), neoxanthin (peak 1), and violaxanthin (peak 2) are the major carotenoids present in leaves of TILLING control (Figure 2d), accounting for 43%, 32%, 13%, and 12%, respectively, of total carotenoids (Table 1). Relative to TILLING control, leaves of *lcye-A*, *lcye-B*, *hyd-A2 hyd-B2*, *lcye-A hyd-A2 hyd-B2*, and *lcye-B hyd-A2 hyd-B2* mutants showed smaller changes in carotenoid profiles than those detected in the mutant combinations including both *lcye-A* and *lcye-B* (Table 1). When either *LCYe-A* or *LCYe-B* were mutated, there was a small but significant decrease (~10%; $P < 0.05$) in lutein as shown in the *lcye-A*, *lcye-B*, *lcye-A hyd-A2 hyd-B2*, and *lcye-B hyd-A2 hyd-B2* mutants. However, when both *LCYe* homoeologs were modified, only a very small peak consistent with the elution time of lutein was observed in the high-performance liquid chromatography (HPLC) chromatograms of *lcye-A lcye-B*, which represents approximately 3% of lutein levels in TILLING control (Figure 2d; Table 1). On the other hand, there was a ~24% increase in β-carotene, a 142% increase in violaxanthin, a ~17% decrease in neoxanthin, and a 19% reduction in total carotenoids in *lcye-A lcye-B* leaves (Table 1). The carotenoid composition and content in *lcye-A lcye-B hyd-A2 hyd-B2* leaves closely resembled those of *lcye-A lcye-B*. Notably, zeaxanthin (peak 5 in Figure 2d) was only detectable in the *lcye-A lcye-B* and *lcye-A lcye-B hyd-A2 hyd-B2* mutants (Table 1).

The carotenoid profile in stems of TILLING control differs from that in leaves with lutein accounting for a higher percentage (49%) of total carotenoids and zeaxanthin accumulating at low levels (1.2%) (Table S1). While the carotenoid profiles of *hyd-A2 hyd-B2* and TILLING control were indistinguishable in stems, lutein content was down by 12%, violaxanthin up by 35%, and β-carotene and neoxanthin were similar in stems of the *lcye-A*, *lcye-B*, *lcye-A hyd-A2 hyd-B2*, and *lcye-B hyd-A2 hyd-B2* mutants relative to TILLING control. Like in leaves, most striking changes in stems were seen in the *lcye-A lcye-B* and *lcye-A lcye-B hyd-A2 hyd-B2* mutants that showed similar levels of decreases in lutein (96%) and neoxanthin (11%), and increases in β-carotene (~24%), violaxanthin (~200%), and zeaxanthin (100%) relative to TILLING control (Table S1).

Mutant plants showed comparable photosynthetic characteristics, but differed in non-photochemical quenching (NPQ) responses, relative to TILLING control

To understand the impact of blocking *LCYe* and *HYD2* on the photosynthetic performance of mutant plants, chlorophyll content and leaf gas exchange of TILLING control and mutants were determined and compared. Total chlorophyll (*Chl*; *Chl* a + b) in *lcye-A lcye-B* and *lcye-A lcye-B hyd-A2 hyd-B2* mutants were reduced by around 10% compared with TILLING control and other mutant genotypes (Table 2; Figure 2d). In addition, the reduction in *Chl a* (peak 7 in Figure 2d) was less than that in *Chl b* (peak 6 in Figure 2d) in *lcye-A lcye-B* and *lcye-A lcye-B hyd-A2 hyd-B2*, which led to an increased *Chl a/b* ratio in these two mutants compared with TILLING control (Table 2). Despite the slight differences in *Chl* ratios in *lcye-A lcye-B* and *lcye-A lcye-B hyd-A2 hyd-B2*, the maximum quantum yield of PSII (F_v/F_m) did not differ significantly ($P > 0.05$) among TILLING control and all mutant genotypes analyzed (Table 2). Stomatal conductance (*Gs*) and internal CO_2 concentrations (*Ci*) were all at a comparable level for TILLING control and mutant plants (Table 2). The net CO_2 assimilation rate (*A*) was similar among TILLNG control and the mutants except for *lcye-A lcye-B* that was decreased by ~11% at a light intensity of 400 μmol m^{-2} s^{-1} (Table 2).

To assess how mutations in *LCYe* and *HYD2* may affect the plant's photoprotective responses under high light stress, the light response of NPQ of chlorophyll fluorescence as well as NPQ induction and relaxation kinetics were determined and compared among TILLING control and the mutants (Figure 3). Similar NPQ responses to light intensities were observed for *lcye-A lcye-B* and *lcye-A lcye-B hyd-A2 hyd-B2*, which were generally less than other mutant genotypes and TILLING control, suggesting a reduced dissipation of excess photosynthetic energy (Figure 3a). At the light intensity of 2,000 μmol m^{-2} s^{-1}, NPQ in *lcye-A lcye-B* and *lcye-A lcye-B hyd-A2 hyd-B2* was ~40% lower than other genotypes (Figure 3a). When NPQ induction kinetics at the light intensity of 1000 μmol m^{-2} s^{-1} were compared, TILLING control, *lcye-B*, *hyd-A2 hyd-B2*, and *lcye-A hyd-A2 hyd-B2* showed the fastest and the highest induction of maximum NPQ (Figure 3b). Both *lcye-A* and *lcye-B hyd-A2 hyd-B2* had a slightly slower response and reached a lower maximum NPQ than TILLING control. Of all mutant genotypes analyzed, *lcye-A lcye-B* and *lcye-A lcye-B hyd-A2 hyd-B2* showed most substantially reduced NPQ induction and maximum levels (Figure 3b). For NPQ relaxation in dark, except for the initial faster relaxation in *lcye-A lcye-B* and *lcye-A lcye-B hyd-A2 hyd-B2* within the first minute to the same level of NPQ as TILLING control and other mutants, all plants maintained the same NPQ level for the next 8 min (Figure 3b).

Table 1 Carotenoid contents (mmol mol^{-1} chlorophylls *a* + *b*) in leaves of TILLING control as well as *lcye-A*, *lcye-B*, *hyd-A2*, and *hyd-B2* mutants and combinations

Genotype	Lutein	β-carotene	Neoxanthin	Violaxanthin	Zeaxanthin	Total
TILLING control	65.73 ± 5.38^{a}	47.75 ± 1.69^{cd}	19.60 ± 0.58^{a}	18.56 ± 2.48^{bc}	ND	151.64 ± 3.22^{a}
lcye-A	58.09 ± 2.40^{b}	50.07 ± 1.06^{b}	18.63 ± 0.40^{bc}	21.51 ± 1.73^{b}	ND	148.30 ± 3.38^{a}
lcye-B	58.42 ± 1.41^{b}	49.52 ± 1.40^{bcd}	19.20 ± 0.38^{abc}	22.02 ± 1.26^{b}	ND	149.17 ± 2.56^{a}
lcye-A lcye-B	1.81 ± 0.12^{c}	59.19 ± 1.02^{a}	16.14 ± 0.40^{d}	44.93 ± 3.37^{a}	10.39 ± 2.06^{a}	122.07 ± 3.90^{b}
hyd-A2 hyd-B2	68.32 ± 1.48^{a}	47.60 ± 0.69^{d}	19.57 ± 0.20^{a}	15.78 ± 1.00^{c}	ND	151.27 ± 2.83^{a}
lcye-A hyd-A2 hyd-B2	58.99 ± 1.91^{b}	49.83 ± 1.86^{bcd}	18.58 ± 0.37^{c}	21.47 ± 2.37^{b}	ND	148.87 ± 3.20^{a}
lcye-B hyd-A2 hyd-B2	59.41 ± 1.75^{b}	49.94 ± 1.79^{bc}	19.21 ± 0.42^{ab}	20.67 ± 2.78^{b}	ND	149.22 ± 3.79^{a}
lcye-A lcye-B hyd-A2 hyd-B2	1.85 ± 0.22^{c}	58.93 ± 1.70^{a}	16.17 ± 0.31^{d}	45.55 ± 4.84^{a}	8.94 ± 4.09^{a}	122.50 ± 6.13^{b}

The carotenoid content was normalized by the content of chlorophylls *a* + *b*. Average values ± SD of 8 biological replicates analyzed for each genotype are shown. Significantly different ($P < 0.05$) values within the same column are indicated with different superscript letters. ND, not detected.

Table 2 Chlorophyll content and photosynthesis-related parameters in leaves of TILLING control as well as *lcye-A*, *lcye-B*, *hyd-A2*, and *hyd-B2* mutants and combinations

Genotype	Chl *a*/*b*	Chl *a* + *b* (μmol g^{-1} fresh tissue)	F_v/F_m	*A* (μmol CO_2 m^{-2} s^{-1})	*Gs* (mol H_2O m^{-2} s^{-1})	C_i (μmol CO_2 mol^{-1} air)
TILLING control	2.61 ± 0.07^{d}	3.70 ± 0.32^{a}	0.837 ± 0.007^{a}	18.18 ± 0.97^{a}	0.48 ± 0.05^{a}	315.22 ± 6.25^{a}
lcye-A	2.70 ± 0.08 cd	3.56 ± 0.19^{ab}	0.835 ± 0.009^{a}	18.18 ± 0.65^{a}	0.52 ± 0.15^{a}	316.67 ± 18.55^{a}
lcye-B	2.62 ± 0.09^{d}	3.71 ± 0.29^{a}	0.833 ± 0.008^{a}	18.27 ± 0.46^{a}	0.54 ± 0.11^{a}	320.94 ± 11.39^{a}
lcye-A lcye-B	2.84 ± 0.06^{a}	3.22 ± 0.11^{b}	0.834 ± 0.013^{a}	16.17 ± 1.30^{b}	0.45 ± 0.06^{a}	319.47 ± 8.50^{a}
hyd-A2 hyd-B2	2.60 ± 0.02^{d}	3.68 ± 0.28^{a}	0.840 ± 0.005^{a}	18.33 ± 0.82^{a}	0.51 ± 0.11^{a}	315.74 ± 13.60^{a}
lcye-A hyd-A2 hyd-B2	2.73 ± 0.08^{bc}	3.40 ± 0.38^{ab}	0.834 ± 0.005^{a}	18.48 ± 0.74^{a}	0.51 ± 0.11^{a}	315.94 ± 11.39^{a}
lcye-B hyd-A2 hyd-B2	2.62 ± 0.04^{d}	3.61 ± 0.23^{ab}	0.836 ± 0.006^{a}	18.07 ± 0.94^{a}	0.52 ± 0.11^{a}	319.41 ± 9.39^{a}
lcye-A lcye-B hyd-A2 hyd-B2	2.83 ± 0.07^{ab}	3.23 ± 0.18^{b}	0.845 ± 0.006^{a}	18.11 ± 0.71^{a}	0.54 ± 0.13^{a}	320.57 ± 13.01^{a}

Photosynthesis-related parameters were measured using LI-6400XT at 400 μmol m^{-2} s^{-1}. Chlorophyll content was measured using high-performance liquid chromatography (HPLC). The average values and standard deviations of 7–9 biological replicates analyzed for each genotype are shown. Significantly different ($P < 0.05$) values within the same column are indicated with different superscript letters. Chl, chlorophyll. *A*, net CO_2 assimilation rate; *Gs*, stomatal conductance; C_i, intercellular CO_2 concentration.

Mutations in LCYe and HYD2 homoeologs have a differential impact on carotenoids in grains than those in leaves

To examine how mutations in *LCYe*, *HYD2*, and their homoeologs affect carotenoid levels in grains, carotenoid content and composition in developing endosperms and mature whole grains were determined (Figures 2b, c, and e; Tables 3, S2, and S3). Endosperms at grain developmental stages 3–5 (i.e. ES3-ES5), corresponding to milky to soft dough stages, were selected for analysis because these grains are amenable to separation of different grain tissues (Qin *et al.*, 2016). Lutein and violaxanthin are the only detectable carotenoids in developing endosperms of TILLING control, *lcye-A*, *lcye-B*, and *lcye-A lcye-B*, and showed reduced accumulation during endosperm development for each plant genotype (Table 3). Although *lcye-A*, *lcye-B*, and *lcye-A lcye-B* all contain less lutein and more violaxanthin relative to TILLING control at the three endosperm developmental stages, this difference is most drastic in *lcye-A lcye-B* where lutein was merely above the threshold for detection by HPLC, violaxanthin was doubled, and total carotenoid content was reduced by 70% at ES5 relative to TILLING control (Table 3).

In contrast to TILLING control, *lcye-A*, *lcye-B*, and *lcye-A lcye-B*, lutein and β-carotene account for all detectable carotenoids in *hyd-A2 hyd-B2*, *lcye-A hyd-A2 hyd-B2*, *lcye-B hyd-A2 hyd-B2*, and *lcye-A lcye-B hyd-A2 hyd-B2* (Table 3). Accompanying decreased lutein accumulation in these *HYD2* deficient mutants (i.e. containing *hyd-A2 hyd-B2* mutations), β-carotene showed increased accumulation when additional *lcye-A* and/or *lcye-B* mutant alleles were incorporated in the *hyd-A2 hyd-B2* background, with 0.67 ± 0.06 μg g^{-1} and 0.76 ± 0.08 μg g^{-1} in ES5 of *lcye-A hyd-A2 hyd-B2* and *lcye-B hyd-A2 hyd-B2*, and 1.55 ± 0.23 μg g^{-1} in ES5 of *lcye-A lcye-B hyd-A2 hyd-B2* (Table 3). It is worth noting that β-carotene and lutein were maintained at similar levels in ES4 and ES5, unlike the decreasing violaxanthin throughout endosperm development of TILLING control, *lcye-A*, *lcye-B*, and *lcye-A lcye-B* (Table 3).

In TILLING control, lutein (~84%; peak 4), zeaxanthin (~12%; peak 5), and β-carotene (~4%; peak 8) were the carotenoids accumulating in mature whole grains (embryo, endosperm, and pericarp of grain development stage 6) (Table S2; Figure 2e). While the *lcye-A* and *lcye-B* single mutants did not differ significantly ($P > 0.05$) from TILLING control, *lcye-A lcye-B* displayed a 95% reduction in lutein, a 60% reduction in zeaxanthin, a similar amount of β-carotene, and an 88% reduction in total carotenoids relative to TILLING control. Mature grains of *hyd-A2 hyd-B2*, *lcye-A hyd-A2 hyd-B2*, and *lcye-B hyd-A2 hyd-B2* were similar in their carotenoid profiles, with doubled β-carotene and moderately reduced lutein and zeaxanthin compared with TILLING control. Although β-carotene was up by 6-fold and reached 1.79 ± 0.18 nmol g^{-1} flour in *lcye-A lcye-B hyd-A2 hyd-B2* when both LCYe and HYD2 activities are blocked, lutein was down to 6%, zeaxanthin to 25%, and total carotenoids to 34% of TILLING control, respectively (Table S2).

Since mature grains are not amenable for dissection of grain components, embryo and pericarp were removed from mature grains through cutting and polishing to assess β-carotene content in endosperm of mature grains (Table S3). Carotenoid composition and content in polished grains of TILLING control and all the mutants largely resemble those in whole grains of these plants as embryo and pericarp only account for a small portion of whole grain by weight (Tables S2 and S3).

Mutations in LCYe and HYD2 homoeologs did not significantly affect seed germination, leaf water content, and grain starch accumulation

To evaluate whether modified carotenoid profiles in grains may affect germination characteristics in the TILLING mutants, spike and seed development was closely monitored and premature seed sprouting was not observed for all mutant plants analyzed (Figure 2a). In addition, seed germination rate was determined and compared between TILLING control and three mutant genotypes with most prominent carotenoid changes, *lcye-A lcye-B*, *hyd-A2 hyd-B2*, and *lcye-A lcye-B hyd-A2 hyd-B2*, for six days (Table S4). Although *hyd-A2 hyd-B2* and *lcye-A lcye-B hyd-A2 hyd-B2* germinated at a slower pace relative to TILLING control, the germination rates were similar for all genotypes tested with approximately 70% germination by day 6 (Table S4). Besides seed germination, rate of leaf water loss was also determined in detached leaves over a 4-h period for TILLING control, and all mutant genotypes, which showed a similar percentage and rate of

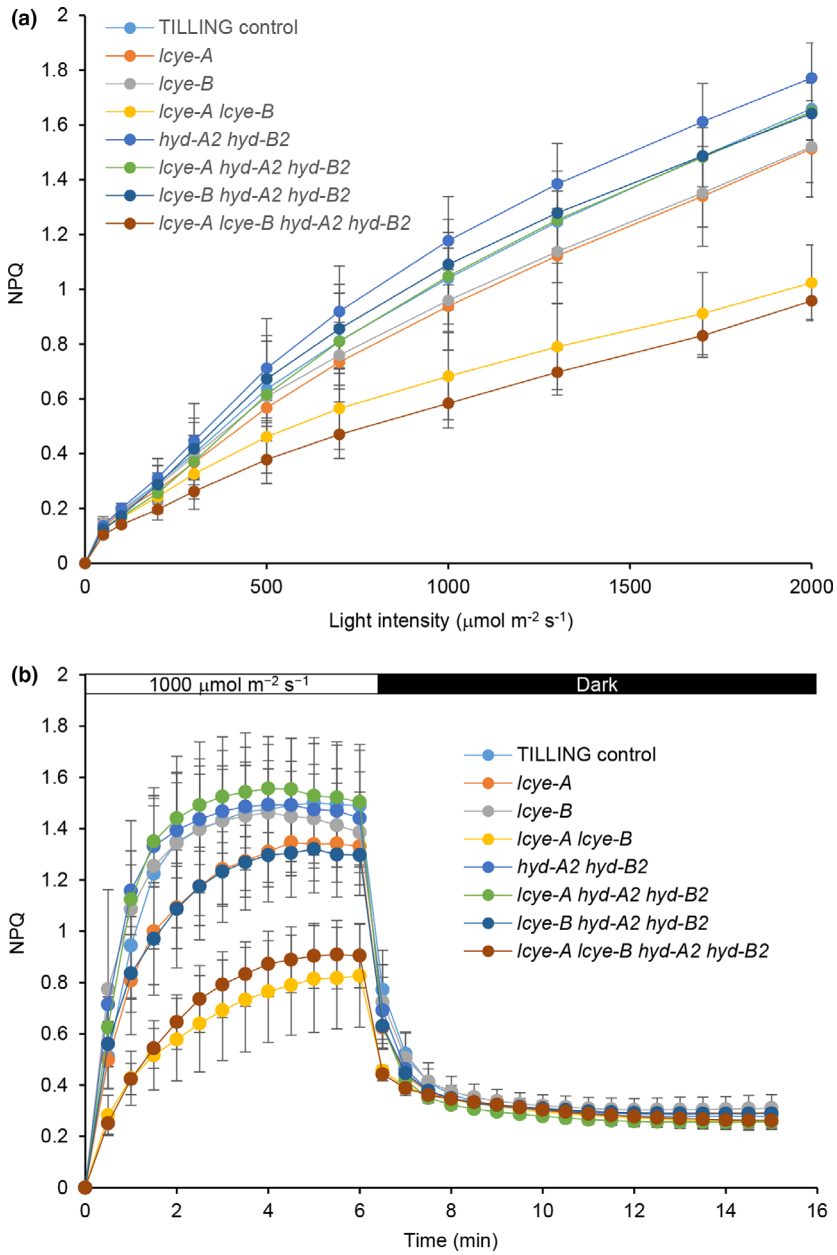

Figure 3 Non-photochemical quenching (NPQ) in leaves of TILLING control as well as *lcye-A*, *lcye-B*, *hyd-A2*, and *hyd-B2* mutants and combinations. (a) Induction of NPQ in dark-adapted leaves at increased light intensities. (b) Induction of NPQ in dark-adapted leaves at 1000 μmol m^{-2} s^{-1} for 6 min followed by relaxation in dark for 9 min. Mean values ± SD of 7–9 independent measurements are shown. SD, standard deviation.

water loss at each time point of measurement (Table S5). To understand whether changes in carotenoids may affect endosperm starch, total starch content of all mutants were determined and shown to be at 55%–60% of total grain weight, comparable to that in TILLING control (Figure S1).

Expression of LCYe and phytoene synthase 1 (PSY1) homoeologs in grain endosperm

The lutein content in ES3-ES5 of *lcye-A* is comparable to that in TILLING control (Table 3), suggesting that there is an active LCYe. To determine whether *LCYe-B* is expressed in developing tetraploid wheat grain endosperms, we used 20% more cDNA template in the real-time qPCR analysis than in our previous study, where *LCYe-B* expression was not reliably detected (Qin *et al.*, 2016). In this study, we detected very low, but above-threshold *LCYe-B* expression in developing endosperms of TILLING control, *lcye-A*, *lcye-B*, and *lcye-A lcye-B* (Figure 4a). In addition, *LCYe-B* expression was not upregulated in *lcye-A* (Figure 4a).

To understand whether the largely decreased total carotenoids in *lcye-A lcye-B* is caused by reduced *PSY1* expression through feedback regulation, *PSY1* homoeolog expression was analyzed and shown that *PSY-A1* and *PSY-B1* expression was not affected by *lcye-A*, *lcye-B*, or *lcye-A lcye-B* mutations in developing endosperms, with the exception of a slight decrease of *PSY-B1* in *lcye-A* and *lcye-B* at ES3 (Figure 4a). *PSY-A1* and *PSY-B1* expression was similar in all vegetative tissues of TILLING control and mutants analyzed (Figure 4b).

Discussion

Taking into consideration the limited natural variation for β-carotene content in wheat, we explored the use of chemical

Table 3 Carotenoid content (nmol g^{-1} fresh tissue) in developing endosperms of wild-type and mutant wheat plants

	Lutein			β-carotene			Violaxanthin			Total		
	ES3	ES4	ES5	ES3	ES4	ES5	ES3	ES4	ES5	ES3	ES4	ES5
TILLING control	6.33 ± 1.40^{a}	4.34 ± 0.90^{a}	4.62 ± 1.13^{a}	ND	ND	ND	2.07 ± 0.45^{c}	1.06 ± 0.26^{c}	0.71 ± 0.22^{c}	8.40 ± 1.58^{ab}	5.41 ± 0.90^{a}	5.33 ± 1.29^{a}
lcye-A	7.13 ± 1.22^{a}	4.14 ± 0.66^{a}	3.82 ± 0.37^{ab}	ND	ND	ND	3.06 ± 0.53^{b}	1.62 ± 0.22^{b}	1.15 ± 0.21^{ab}	10.19 ± 1.73^{a}	5.76 ± 0.79^{a}	4.97 ± 0.54^{ab}
lcye-B	4.69 ± 0.28^{b}	2.96 ± 0.28^{b}	2.90 ± 0.16^{bc}	ND	ND	ND	3.38 ± 0.33^{b}	1.92 ± 0.16^{ab}	1.02 ± 0.17^{bc}	8.07 ± 0.44^{b}	4.88 ± 0.34^{a}	3.92 ± 0.18^{bc}
lcye-A lcye-B	0.40 ± 0.08^{e}	0.31 ± 0.05^{d}	0.28 ± 0.06^{d}	ND	ND	ND	4.88 ± 0.67^{a}	2.38 ± 0.57^{a}	1.39 ± 0.34^{a}	5.28 ± 0.72^{c}	2.69 ± 0.59^{b}	1.66 ± 0.39^{e}
hyd-A2 hyd-B2	4.18 ± 0.17^{bc}	2.93 ± 0.17^{b}	2.44 ± 0.31^{c}	0.66 ± 0.02^{c}	0.46 ± 0.01^{c}	0.48 ± 0.02^{c}	ND	ND	ND	4.84 ± 0.18^{c}	3.39 ± 0.17^{b}	2.91 ± 0.33 cd
lcye-A hyd-A2 hyd-B2	3.22 ± 0.40 cd	2.53 ± 0.17^{bc}	2.19 ± 0.29^{c}	0.88 ± 0.07^{b}	0.66 ± 0.03^{b}	0.67 ± 0.06^{b}	ND	ND	ND	4.10 ± 0.48 cd	3.19 ± 0.19^{b}	2.86 ± 0.33 cd
lcye-B hyd-A2 hyd-B2	2.74 ± 0.31^{d}	1.98 ± 0.15^{c}	2.53 ± 0.49^{c}	0.86 ± 0.04^{b}	0.61 ± 0.05^{b}	0.76 ± 0.08^{b}	ND	ND	ND	3.60 ± 0.33 cd	2.60 ± 0.19^{b}	3.29 ± 0.52^{c}
lcye-A lcye-B hyd-A2 hyd-B2	0.38 ± 0.14^{e}	0.22 ± 0.03^{d}	0.21 ± 0.04^{d}	2.25 ± 0.17^{a}	1.55 ± 0.10^{a}	1.55 ± 0.23^{a}	ND	ND	ND	2.62 ± 0.26^{d}	1.77 ± 0.11^{c}	1.77 ± 0.27^{de}

The average values and standard deviations of 4–5 biological replicates are shown. Significantly different ($P < 0.05$) values within the same column are indicated with different superscript letters. ES3, ES4, ES5, endosperms at grain developmental stages 3, 4, 5; ND, not detected.

mutagenesis to understand and manipulate carotenoid metabolism in the grain endosperm for provitamin A biofortification in tetraploid wheat. Consistent with the results from our spatial gene expression analysis (Qin *et al*., 2016), eliminating HYD2 activities successfully inhibited the transformation of β-carotene to xanthophylls in developing endosperms of *hyd-A2 hyd-B2*, as demonstrated by their lack of violaxanthin and increased β-carotene accumulation (Table 3). On the other hand, carotenoid profiles were similar in leaves and stems of *hyd-A2 hyd-B2* and TILLING control, suggesting that the functional loss of HYD2 can be compensated by HYD1 in the vegetative tissues (Tables 1 and S1).

Contrasting the complementary function of HYD1 and HYD2, the ~10% reduced lutein in leaves and stems of the *lcye-A* and *lcye-B* single mutants suggests that LCYe-A and LCYe-B can only partially compensate for each other's activity in these tissues (Tables 1 and S1). However, the photosynthetic properties of *lcye-A* and *lcye-B* were similar to those of TILLING control, indicating that the slightly reduced lutein does not affect the performance of these mutant plants under the conditions tested in this study (Figure 3; Table 2). In developing endosperm of TILLING control seeds, the expression of *LCYe-B* was extremely low and at only ~10% of *LCYe-A* transcript levels (Figure 4a). In addition, *LCYe-B* expression was not induced by the *lcye-A* mutation in endosperms of *lcye-A* (Figure 4a). Taken together, these results suggest that *LCYe-B* transcripts in *lcye-A*, though at low abundance, are effectively translated into LCYe-B proteins capable of producing lutein to a level similar to that in TILLING control (Figure 4a; Table 3).

While β-carotene was not detectable in ES5 (late developmental stage of endosperm) of TILLING control, the accumulation of β-carotene reached 0.48 ± 0.02 nmol g^{-1} in ES5 of *hyd-A2 hyd-B2*, and was further enhanced to 0.67 ± 0.06, 0.76 ± 0.08, and 1.55 ± 0.23 nmol g^{-1} in ES5 of *lcye-A hyd-A2 hyd-B2*, *lcye-B hyd-A2 hyd-B2*, and *lcye-A lcye-B hyd-A2 hyd-B2*, respectively, indicating that the combination of redirecting lutein biosynthesis and reducing β-carotene turnover to xanthophylls effectively enriches β-carotene in tetraploid wheat endosperm [Table 3; note that β-carotene in the endosperm is not significantly ($P < 0.05$) different between *lcye-A hyd-A2 hyd-B2* and *lcye-B hyd-A2 hyd-B2*]. These results provide a possible pathway to provitamin A enrichment in wheat grains.

β-carotene-derived xanthophylls serve as biosynthetic precursors of abscisic acid (ABA) (Figure 1a). Seed germination and leaf water loss assays revealed similar performance of *lcye-A hyd-A2 hyd-B2*, *lcye-B hyd-A2 hyd-B2*, *lcye-A lcye-B hyd-A2 hyd-B2*, and TILLING control for physiological processes controlled by ABA (Tables S4–S5). These results suggest that ABA is still adequately produced in these triple and quadruple mutants as β-carotene-derived xanthophylls accumulate in leaves (neoxanthin and violaxanthin) and whole grains (zeaxanthin) (Tables 1 and S2). Although the triple and quadruple mutants and TILLING control exhibited similar photosynthetic performance at 400 μmol m^{-2} s^{-1} (Table 2), only *lcye-A hyd-A2 hyd-B2* did not differ from TILLING control in light response of photosynthesis and NPQ induction (Figure 3), demonstrating that this triple mutant combination succeeded in achieving increased β-carotene content in the endosperm without having an impact on photosynthesis. We are currently increasing seeds to evaluate these lines in the field to quantify potential pleiotropic effects of these mutations on agronomic traits.

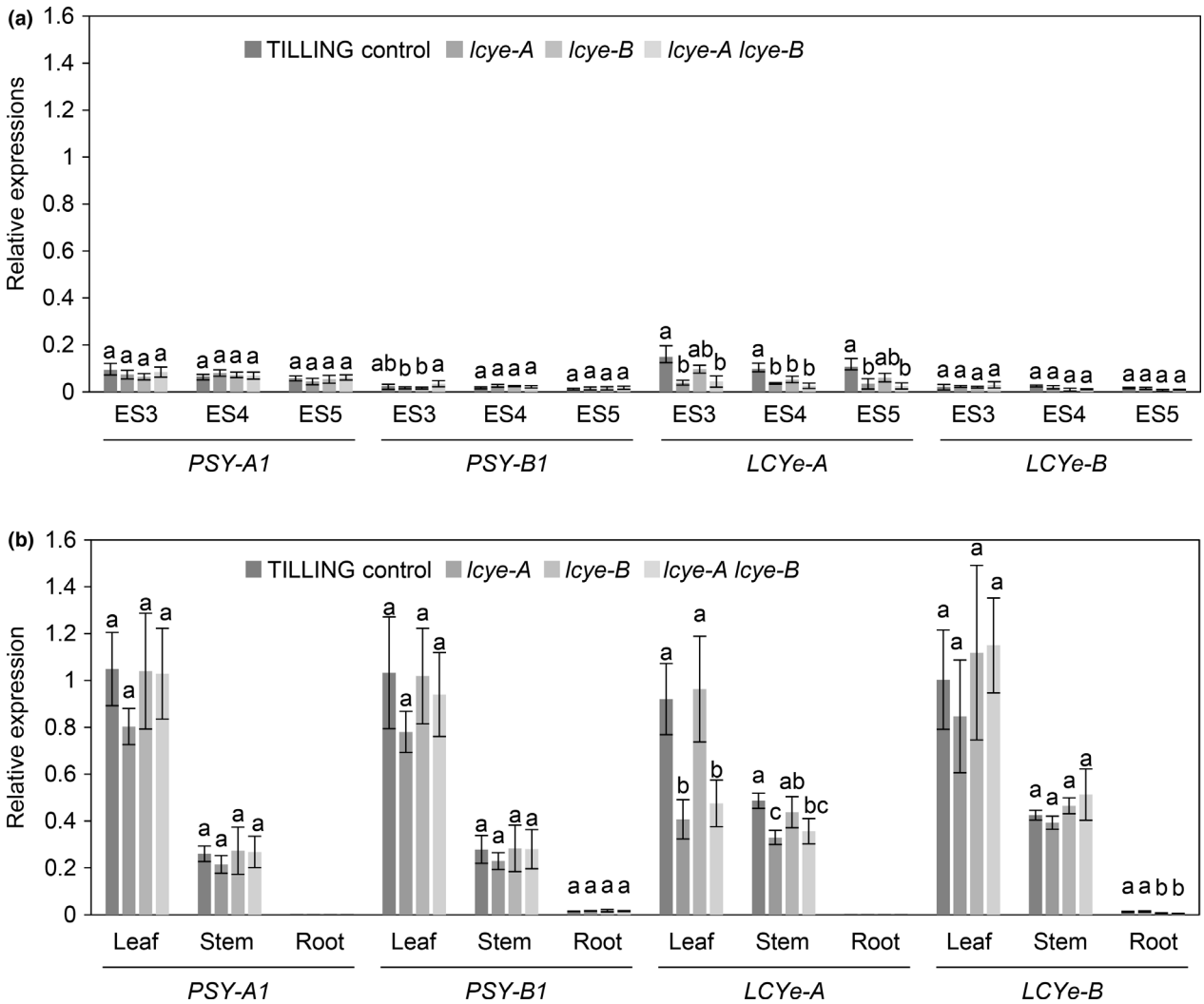

Figure 4 Relative expression of *PSY1* and *LCYe* homoeologs in tetraploid wheat vegetative tissues and developing grain endosperms of TILLING control as well as *lcye-A*, *lcye-B*, and *lcye-A lcye-B* mutants. (a) Relative expression of *PSY1* and *LCYe* homoeologs in endosperms at grain developmental stages 3–5 (ES3-ES5). (b) Relative expression of *PSY1* and *LCYe* homoeologs in leaves, stems and roots. Transcript quantification was conducted using the relative standard curve method (Applied Biosystems, 2004). The geometric mean of two reference genes, *Ta2291* and *Ta54227*, was used for normalization of gene expression. Values shown are the mean ± SD of 4 biological replicates. Significant differences ($P < 0.05$) in Tukey's HSD test for each tissue type or endosperm developmental stage are denoted by different letters.

When both LCYe-A and LCYe-B are suppressed in *lcye-A lcye-B*, the drastic loss of lutein did not lead to an equivalent increase in β-carotene and its derived carotenoids, but rather a reduction in total carotenoids was observed in developing endosperms (~70% reduction at ES5) and whole grains (~88% reduction) (Tables 3 and S2). *PSY-A1* and *PSY-B1* were expressed similarly in endosperms of TILLING control and *lcye-A lcye-B* (Figure 4A), suggesting that reduction in total carotenoids in *lcye-A lcye-B* may not be due to feedback regulation of the early pathway step catalyzed by PSY (Figure 1A). It also suggests that, though carbon flux is directed from lutein to β-carotene biosynthesis by blocking LCYe, β-carotene, and/or its xanthophyll derivatives could be removed by additional activities, such as carotenoid cleavage dioxygenases (CCDs). In contrast to the ~70% reduced total carotenoids in endosperms, only 20% decrease in total carotenoids was observed in leaves and stems of *lcye-A lcye-B* (Tables 1 and S1), indicating different processes likely exist in vegetative tissues and grains. Previous *in vitro* enzyme assays showed that wheat CCD1, not CCD4, could use β-carotene as substrate (violaxanthin was not tested) with low efficiency and *CCD-A1*, but not *CCD-B1* and *CCD4* homoeologs, was expressed in endosperms (Qin *et al*., 2016), further pinpointing CCD-A1 as the potential activity for cleaving β-carotene and β-carotene-derived xanthophylls into apocarotenoids. However, overexpression of *OsCCD1* in Golden Rice endosperm did not affect carotenoid content in one study (Ilg *et al*., 2010), and a similar experiment in a different Golden Rice background led to up to 1.4-fold higher grain carotenoid accumulation with very little change in β-carotene content in another study (Ko *et al*., 2018). It remains to be determined whether eliminating *CCD1* activity could further increase β-carotene in endosperms of mutant combinations with blocked LCYe and HYD2 activities.

Going forward, a few strategies could be deployed to enhance β-carotene in *lcye-B hyd-A2 hyd-B2*. It was previously shown that

wheat *PSY1* is tightly associated with the major GYPC QTL on Chromosome 7 (He *et al*., 2008; Howitt *et al*., 2009). Natural and induced allelic variations in *PSY1* sequences correlate with carotenoid pigment content in tetraploid and hexaploid wheat grains, demonstrating that *PSY1* is the underlying gene for this QTL (He *et al*., 2008; Zhang and Dubcovsky, 2008). *PSY1* alleles contributing to high carotenoid accumulation could be stacked to *lcye-B hyd-A2 hyd-B2* through breeding to further increase the accumulation of β-carotene and total carotenoids. In this regard, a *PSY-B1* allele generated by a conversion event between *PSY-B1* and *PSY-A1* with increased yellow pigment has been already identified in the tetraploid variety Kofa (Zhang and Dubcovsky, 2008). Additionally, recent studies with the cauliflower Orange (*Or*) mutant and Or proteins in different plants also point to the promising avenue of improving β-carotene sequestration in provitamin A biofortified wheat grains (Sun *et al*., 2020; Watkins and Pogson, 2020).

Our comparative analysis of *lcye* and *hyd2* mutant combinations provided new insights to carotenoid metabolism in tetraploid wheat grains. When transgenic approaches become more broadly accepted by the public, endosperm-specific expression of RNA interference constructs against *LCYe* and *HYD2* using the high-molecular-weight glutenin promoter (Bregitzer *et al*., 2006; Lamacchia *et al*., 2001) offers the opportunity to knockout these genes to enrich β-carotene in endosperm while maintaining carotenoid profile and function in other tissues as well as normal plant growth. After the effects of the *lcye* and *hyd2* mutations on agronomic traits are evaluated in field experiments, TILLING mutant combinations with adequate agronomic performance can be directly incorporated in breeding (e.g. with high carotenoid producing *PSY1* alleles) to generate wheat cultivars with increased β-carotene. This study also sets the stage for a gene editing-based approach for provitamin A biofortification in hexaploid wheat.

Experimental procedures

Plant growth and tissue collection

Wheat seeds were disinfected with 1% (w/v) sodium hypochlorite and 0.1% (v/v) Triton X-100 for 15 min and rinsed three times with water. Sterilized seeds were kept at 4 °C for 3 days and then at room temperature in dark for 2–4 days to develop roots. Germinated seeds were then planted in soil or vermiculate and grown in a temperature-controlled greenhouse at 400 μmol m^{-2} s^{-1} in a long day photoperiod (16 h light/8 h dark).

For carotenoid and chlorophyll analysis of vegetative tissues, the fourth leaf from the top of the primary tillers and stem were collected from four-week-old, soil-grown plants. For gene expression analysis, leaf, stem, and root tissues were collected from four-week-old vermiculite-grown plants. For carotenoid analysis of developing endosperms, whole grains were harvested at developmental stages 3–5 as previously defined and described (Qin *et al*., 2012) and dissected using a scalpel. Endosperms collected from grains in the same spike were pooled and considered a biological replicate. For carotenoid analysis of mature whole grains, spikes were harvested when kernels could not be dented by a thumbnail. The spikes were dried at room temperature for one week and grains were separated from chaff by hand. For carotenoid analysis of polished grains, embryos were removed from mature whole grains using a razor blade, which were then polished between two pieces of sand paper. All tissues described above, except for mature whole/polished grains, were frozen immediately in liquid nitrogen upon collection, ground into fine powder in liquid nitrogen using a mortar and pestle, and stored at −80 °C until analysis.

Isolation, backcrossing, and intercrossing of wheat TILLING mutants

Mutants of carotenoid metabolic gene homoeologs were identified from a tetraploid wheat cv Kronos TILLING mutant library using a combination of non-denaturing polyacrylamide gel-based method (Uauy *et al*., 2009) and searching the wheat TILLING mutant database when mutant sequences became available (Krasileva *et al*., 2017). Primers used for wheat TILLING mutant screening are listed in Table S6. Putative loss-of-function TILLING mutant lines for *LCYe-A* (T4-2426), *LCYe-B* (T4-2543), *HYD-A2* (T4-0870), and *HYD-B2* (T4-4420) were designated *lcye-A*, *lcye-B*, *hyd-A2*, and *hyd-B2*, respectively, and used in this study.

The above-mentioned TILLING mutants were each backcrossed to the wild-type parental line Kronos two times to remove ~75% of background mutations caused by chemical mutagenesis. Background-purified single TILLING mutants were intercrossed and genotyped to identify double mutants of the *LCYe* or *HYD2* homoeologs, that is the *lcye-A lcye-B* and *hyd-A2 hyd-B2* mutants. *Hyd-A2 hyd-B2* and *lcye-A lcye-B* mutants were crossed and several of the resulting heterozygous quadruple mutant plants (heterozygous for the *LCYe-A*, *LCYe-B*, *HYD-A2*, and *HYD-B2* loci) were self-pollinated and grown into mature plants; this is to ensure that a sufficient amount of seeds would be obtained in the segregating population for identification of homozygous quadruple mutants. The segregating progenies were genotyped for the *LCYe-A*, *LCYe-B*, *HYD-A2*, and *HYD-B2* loci to identify various mutant combinations. Segregants possessing wild-type alleles for all four loci (i.e. *LCYe-A LCYe-B HYD-A2 HYD-B2*) contain a similar level of background mutations as the mutants; they were used as TILLING control for all analyses described in this study.

For identification of wild-type and mutant alleles of *LCYe-A*, *LCYe-B*, *HYD-A2*, and *HYD-B2* in the backcrossed and intercrossed progenies, genomic DNA was isolated from the leaf tissue using a high-throughput DNA extraction method (Pallotta *et al*., 2003). Cleaved Amplified Polymorphic Sequences (CAPS) or derived CAPS (dCAPS) markers (Neff *et al*., 2002) were designed for the *lcye-A*, *lcye-B*, *hyd-A2*, and *hyd-B2* mutation. PCR primers and restriction enzymes (New England Biolabs, Ipswich, MA) used in the CAPS and dCAPS analyses are shown in Table S6. PCR products were digested with the corresponding restriction enzymes at 37 °C for 2 h or overnight and separated on a 2.5% agarose gel.

Leaf gas exchange and chlorophyll fluorescence measurements

A LI-6400XT portable photosynthesis system (LI-COR Biosciences, Lincoln, NE) connected with a 6400-40 leaf chamber fluorometer was used to measure leaf gas exchange and chlorophyll fluorescence. Light-adapted flag leaves at the grain filling stage were used to determine stomatal conductance (G_s), net CO_2 assimilation rate (A), and intercellular CO_2 concentration (C_i) during the day. Leaf temperature was set at 25 °C and the air flow rate in the chamber was maintained at 200 μmol s^{-1}. The concentration of reference CO_2 remained constant at 400 μmol mol^{-1}. The internal light-emitting diode (LED) light source was set at 400 μmol m^{-2} s^{-1} with 90% red light and 10% blue light.

Chlorophyll fluorescence measurements were performed at 25 °C on flag leaves that had been dark-adapted overnight.

Minimal dark-adapted fluorescence (F_0), maximal dark-adapted fluorescence (F_m), steady state light-adapted fluorescence (F_s), minimal light-adapted fluorescence (F_0'), and maximal light-adapted fluorescence (F_m') were determined. The maximum quantum yield of photosystem II (PSII) and non-photochemical quenching (NPQ) were calculated as $F_v/F_m = (F_m–F_0)/F_m$ and $(F_m–F_m')/F_m'$, respectively.

To determine light response of NPQ, flag leaves were illuminated at the light intensity of 50, 100, 200, 300, 500, 700, 1000, 1300, 1700, and 2000 μmol m^{-2} s^{-1}. To determine NPQ induction and relaxation kinetics, a saturating light pulse was applied to dark-adapted leaves followed immediately by a non-saturating actinic light of 1000 μmol m^{-2} s^{-1}. Saturating pulses were then applied every 30 s and the actinic light was turned off after 6 min. Saturating pulses were applied every 30 s for an additional 9 min to determine relaxation of NPQ.

Carotenoid and chlorophyll analysis

Extraction of carotenoids and chlorophylls was carried out at room temperature under dimmed light. At least four biological replicates were used for TILLING control and each mutant genotype analyzed. To leaf (~50 mg), stem (~200 mg) or endosperm (~200 mg) tissues, 900 μL of acetone: ethyl acetate (3:2, v/v) and 1.8 μg of β-apo-8′-carotenal internal standard were added. The mixture was incubated in dark for 1 h, with intermittent mixing at every 15 min, followed by addition of 400 μL of H_2O. After centrifugation at 13 000 rpm for 5 min, the upper ethyl acetate layer was transferred to an HPLC vial and 10 μL of the extract was used for HPLC analysis as described (Qin *et al.*, 2012).

Mature grains harvested from the same wheat plant were divided into two aliquots. While grains in one aliquot were ground and used directly for carotenoid extraction (to obtain whole grain flour), grains in the other aliquot had embryos removed with a razor blade, were polished using sand paper, and were ground into flour (to obtain polished grain flour). Whole or polish grain flour (~300 mg) was rehydrated in 300 μL of H_2O and then extracted using 3 mL of methanol and 3 mL of diethyl ether with 1.5 μg of β-apo-8′-carotenal as internal standard. The pooled methanol and diethyl ether extracts were partitioned with 4.5 mL of H_2O; the lower phase was re-extracted with 1.5 mL of diethyl ether for two times. The diethyl ether fractions were combined and dried under a stream of nitrogen gas. The carotenoids were saponified in 2 M KOH [dissolved in methanol with 0.01% (w/v) butylated hydroxytoluene] in dark for 30 min, followed by phase separation using equal volumes of diethyl ether and H_2O (2 mL for each). The water phase was re-extracted with 2 mL of diethyl ether for three times. The diethyl ether layers were pooled, washed twice with 6 mL of H_2O, and dried under nitrogen gas. Carotenoid residues were dissolved in 300 μL of ethyl acetate and partitioned by adding 250 μL of H_2O. After separating by centrifugation, the ethyl acetate layer was transferred to an HPLC vial and 10 μL of the extract was used for HPLC analysis as described (Qin *et al.*, 2012).

Real-time qPCR analysis

Total RNA was isolated from leaf, stem, and root tissues (~50 mg) using TRIzol reagent (Invitrogen, Carlsbad, CA) and from developing endosperms (~100 mg) using a cetyltrimethylammonium bromide (CTAB)-based method. After treating with DNase I (Thermo Scientific, Waltham, MA), total RNA (1.2 μg) was subjected to the synthesis of first-strand cDNA using the iScript Advanced cDNA Synthesis Kit (BioRad, Hercules, CA) following manufacturer's instructions.

Real-time qPCR analysis was carried out on an ABI Prism® 7300 Real-time qPCR system (Applied Biosystems, Foster City, CA) as previously described (Qin *et al.*, 2012). The total volume of the qPCR mix was 20 μL, containing 0.27 μL of cDNA, 200 nM each primer, and 1× iTaq SYBR® Green Supermix (BioRad). Primers used for the real-time qPCR analysis are listed in Table S7. The forward primer of *LCYe-A* is located in the last exon and the reverse primer hybridizes in the 3′-untranslated region (3′-UTR). Both forward and reverse primers of *LCYe-B* are located in the 3′-UTR. Four biological replicates, each with three technical replicates, were used in the gene expression analysis of TILLING control and mutant plants. Relative gene expression in different tissues was determined using the relative standard curve method. Standard curves were prepared with serial dilutions of cDNAs synthesized from total RNA extracted from leaves of TILLING control. The geometric mean of two reference genes, *Ta2291* and *Ta54227*, was used for normalization of gene expression in different tissues.

Leaf water loss and seed germination analyses

Four-week-old mutant and TILLING control plants were used in the leaf water loss analysis. The third leaf from the top on the primary tiller of each plant was detached. The detached leaves were weighted every 60 min for a total of 240 min. The rate of water loss was calculated as the loss of weight in percentage. There were 9 biological replicates for TILLING control and each mutant genotype.

Healthy and clean seeds collected from the same wheat plant were pooled, from which 50 seeds were randomly selected and used for determination of seed germination rate. Seeds were surface-sterilized as described above, transferred to a petri dish (100 mm × 100 mm) bedded with two pieces of damp Waterman filter paper, and kept in dark at room temperature. The number of germinated seeds was recorded daily for 6 days and the percentage of germinated seeds was calculated. This experiment was repeated for 3–5 times for TILLING control and the mutants.

Starch analysis

Starch in 100 mg of whole grain flour was extracted and analyzed using the Megazyme Total Starch Assay kit (Megazyme, County Wicklow, Ireland). In each analysis, there were 4 biological replicates for TILLING control and each mutant genotype.

Statistical analysis

The one-way analysis of variance (ANOVA) analysis was performed using R (R Core Team). Mean comparisons were performed with Tukey's Honestly Significant Difference (HSD) test.

Acknowledgements

The authors thank Drs. Heiner Lieth and Matthew Gilbert for providing us access to the LI-6400XT Portable Photosynthesis System and also thank Cody Bekkering for critical reading of the manuscript.

Conflict of interest

The authors declare no competing interests.

Funding

This work was funded by USDA-NIFA to L.T. (2017-67013-26164). J.D. acknowledges support by the Howard Hughes Medical Institute and Betty and Gordon Moore Foundation. S.Y. was supported by a China Scholarship Council Scholarship, the Henry A. Jastro Research Award, and the UC Davis Department of Plant Sciences Graduate Research Fellowship.

Author contributions

L.T. conceived of the project; S.Y. and L.T. designed the experiments; J.D. provided wheat TILLING mutant materials; S.Y. identified the TILLING mutants and performed crossing; S.Y. and M.L. performed the genotyping; S.Y. characterized the TILLING mutant combinations; S.Y., J.D., and L.T. analyzed the data; S.Y. and L.T. wrote the manuscript; all authors reviewed and commented on the manuscript.

Data availability statement

All relevant data can be found within the manuscript and its Supporting Information.

References

Applied Biosystems. (2004). *Guide to performing relative quantitation of gene expression using Real-Time quantitative PCR*.

Bouvier, F., Keller, Y., d'Harlingue, A. and Camara, B. (1998) Xanthophyll biosynthesis: molecular and functional characterization of carotenoid hydroxylases from pepper fruits (*Capsicum annuum* L.). *Biochim. Biophys. Acta*, **1391**, 320–328.

Bregitzer, P., Blechl, A.E., Fiedler, D., Lin, J., Sebesta, P., De Soto, J.F., Chicaiza, O. and *et al*. (2006) Changes in high molecular weight glutenin subunit composition can be genetically engineered without affecting wheat agronomic performance. *Crop. Sci.* **46**, 1553–1563.

Britton, G. (2009) Vitamin A and vitamin A deficiency. In: *Carotenoids. Volume 5: Nutrition and Health* (Britton, G., Liaaen-Jensen, S. and Pfander, H. eds). pp. 173–190. Basel: Birkhäuser Verlag.

Cunningham, F., Pogson, B., Sun, Z., McDonald, K., DellaPenna, D. and Gantt, E. (1996) Functional analysis of the beta and epsilon lycopene cyclase enzymes of Arabidopsis reveals a mechanism for control of cyclic carotenoid formation. *Plant Cell*, **8**, 1613–1626.

Diretto, G., Tavazza, R., Welsch, R., Pizzichini, D., Mourgues, F., Papacchioli, V., Beyer, P. and *et al*. (2006) Metabolic engineering of potato tuber carotenoids through tuber-specific silencing of lycopene epsilon cyclase. *BMC Plant Biol.* **6**, 13.

Diretto, G., Welsch, R., Tavazza, R., Mourgues, F., Pizzichini, D., Beyer, P. and Giuliano, G. (2007) Silencing of beta-carotene hydroxylase increases total carotenoid and beta-carotene levels in potato tubers. *BMC Plant Biol.* **7**, 11.

Harjes, C., Rocheford, T., Bai, L., Brutnell, T., Kandianis, C., Sowinski, S., Stapleton, A. *et al* .*et al*.(2008) Natural genetic variation in lycopene epsilon cyclase tapped for maize biofortification. *Science*, **319**, 330–333.

He, X., Zhang, Y., He, Z., Wu, Y., Xiao, Y., Ma, C. and Xia, X. (2008) Characterization of phytoene synthase 1 gene (*Psy1*) located on common wheat chromosome 7A and development of a functional marker. *Theor. Appl. Genet.* **116**, 213–221.

Howitt, C., Cavanagh, C., Bowerman, A., Cazzonelli, C., Rampling, L., Mimica, J. and Pogson, B. (2009) Alternative splicing, activation of cryptic exons and amino acid substitutions in carotenoid biosynthetic genes are associated with lutein accumulation in wheat endosperm. *Funct. Integr. Genomics*, **9**, 363–376.

Ilg, A., Yu, Q., Schaub, P., Beyer, P. and Al-Babili, S. (2010) Overexpression of the rice *carotenoid cleavage dioxygenase 1* gene in Golden Rice endosperm suggests apocarotenoids as substrates *in planta*. *Planta*, **232**, 691–699.

Ko, M.R., Song, M.-H., Kim, J.K., Baek, S.-A., You, M.K., Lim, S.-H. and Ha, S.-H. (2018) RNAi-mediated suppression of three carotenoid-cleavage dioxygenase genes, *OsCCD1*, *4a*, and *4b*, increases carotenoid content in rice. *J. Exp. Bot.* **69**, 5105–5116.

Krasileva, K.V., Vasquez-Gross, H.A., Howell, T., Bailey, P., Paraiso, F., Clissold, L., Simmonds, J. *et al*. (2017) Uncovering hidden variation in polyploid wheat. *Proc. Natl. Acad. Sci. U.S.A.*, **114**, E913–E921.

Lamacchia, C., Shewry, P.R., Di Fonzo, N., Forsyth, J.L., Harris, N., Lazzeri, P.A., Napier, J.A. *et al*. (2001) Endosperm-specific activity of a storage protein gene promoter in transgenic wheat seed. *J. Exp. Bot.* **52**, 243–250.

Mora, J.R., Iwata, M. and von Andrian, U.H. (2008) Vitamin effects on the immune system: vitamins A and D take centre stage. *Nat. Rev. Immunol.* **8**, 685–698.

Neff, M.M., Turk, E. and Kalishman, M. (2002) Web-based primer design for single nucleotide polymorphism analysis. *Trends Genet*, **18**, 613–615.

Paine, J.A., Shipton, C.A., Chaggar, S., Howells, R.M., Kennedy, M.J., Vernon, G., Wright, S.Y. *et al*. (2005) Improving the nutritional value of Golden Rice through increased pro-vitamin A content. *Nat. Biotechnol.* **23**, 482–487.

Pallotta, M., Warner, P., Fox, R., Kuchel, H., Jefferies, S. and Langridge, P. (2003) *Marker assisted wheat breeding in the southern region of Australia*. In: Proceedings of the 10th International Wheat Genetics Symposium Paestum, Italy. 789-791.

Qin, X., Fischer, K., Yu, S., Dubcovsky, J. and Tian, L. (2016) Distinct expression and function of carotenoid metabolic genes and homoeologs in developing wheat grains. *BMC Plant Biol.* **16**, 155.

Qin, X., Zhang, W., Dubcovsky, J. and Tian, L. (2012) Cloning and comparative analysis of carotenoid β-hydroxylase genes provides new insights into carotenoid metabolism in tetraploid (*Triticum turgidum* ssp. *durum*) and hexaploid (*Triticum aestivum*) wheat grains. *Plant Mol. Biol.* **80**, 631–646.

Richaud, D., Stange, C., Gadaleta, A., Colasuonno, P., Parada, R. and Schwember, A.R. (2018) Identification of *Lycopene epsilon cyclase* (*LCYE*) gene mutants to potentially increase β-carotene content in durum wheat (*Triticum turgidum* L. ssp. *durum*) through TILLING. *PLoS One*, **13**, e0208948.

Sestili, F., Garcia-Molina, M.D., Gambacorta, G., Beleggia, R., Botticella, E., De Vita, P., Savatin, D.V. *et al*. (2019) Provitamin A biofortification of durum wheat through a TILLING approach. *Int. J. Mol. Sci.* **20**, 5703.

Shumskaya, M. and Wurtzel, E.T. (2013) The carotenoid biosynthetic pathway: thinking in all dimensions. *Plant Sci.* **208**, 58–63.

Sun, T., Tadmor, Y. and Li, L. (2020). Pathways for carotenoid biosynthesis, degradation, and storage. In *Plant and food carotenoids: Methods and protocols* (Rodríguez-Concepción, M. and Welsch, R., eds). pp. 3-23. New York, NY: Springer US.

Uauy, C., Paraiso, F., Colasuonno, P., Tran, R., Tsai, H., Berardi, S., Comai, L. and *et al*. (2009) A modified TILLING approach to detect induced mutations in tetraploid and hexaploid wheat. *BMC Plant Biol.* **9**, 115.

Watkins, J.L. and Pogson, B.J. (2020) Prospects for carotenoid biofortification targeting retention and catabolism. *Trends Plant Sci.* **25**, 501–512.

Yan, J., Kandianis, C., Harjes, C., Bai, L., Kim, E., Yang, X., Skinner, D. *et al*. (2010) Rare genetic variation at *Zea mays crtRB1* increases beta-carotene in maize grain. *Nat. Genet.* **42**, 322–327.

Ye, X., Al-Babili, S., Klöti, A., Zhang, J., Lucca, P., Beyer, P. and Potrykus, I. (2000) Engineering the provitamin A (β-carotene) biosynthetic pathway into (carotenoid-free) rice endosperm. *Science*, **287**, 303–305.

Yu, B., Lydiate, D., Young, L., Schäfer, U. and Hannoufa, A. (2008) Enhancing the carotenoid content of *Brassica napus* seeds by downregulating lycopene epsilon cyclase. *Transgenic Res.* **17**, 573–585.

Yu, S. and Tian, L. (2018) Breeding major cereal grains through the lens of nutrition sensitivity. *Mol. Plant*, **11**, 23–30.

Zhang, W. and Dubcovsky, J. (2008) Association between allelic variation at the *Phytoene synthase 1* gene and yellow pigment content in the wheat grain. *Theor. Appl. Genet.* **116**, 635–645.

Supporting information

Additional supporting information may be found online in the Supporting Information section at the end of the article.

Figure S1. Total starch content in whole grains of TILLING control as well as *lcye-A*, *lcye-B*, *hyd-A2*, and *hyd-B2* mutants and combinations.
Table S1. Carotenoid contents (mmol mol^{-1} chlorophylls *a* + *b*) in stems of TILLING control and mutant wheat plants.
Table S2. Carotenoid content (nmol g^{-1} flour) in whole grains of wild-type and mutant wheat plants.
Table S3. Carotenoid content (nmol g^{-1} flour) in polished whole grains of wild-type and mutant wheat plants.
Table S4. Germination rate and percentage of TILLING control and mutants.
Table S5. Leaf water loss of TILLING control and mutant plants.
Table S6. CAPS and dCAPS markers used for genotyping of wild-type and mutant *LCYe-A*, *LCYe-B*, *HYD-A2*, and *HYD-B2* alleles.
Table S7. Sequences of homoeolog-specific primers used in the real-time qPCR analysis.

